Hydraulic Model Investigation of a Two-Way Drop Inlet For Floodwater Retarding Structure No. 3 Banklick Creek Watershed, Boone and Kenton Counties, Kentucky

NORTH CENTRAL
REGION

SCIENCE AND EDUCATION ADMINISTRATION • U.S. DEPARTMENT OF AGRICULTURE

With this issue, the ARS-NC series (and SEA-NC 59, 61, 62) published
from July 1972 to March 1978 by the Agricultural Research Service,
North Central Region, Peoria, Ill.   61614, is discontinued.

On January 24, 1978, four U.S. Department of Agriculture agencies—
Agricultural Research Service,
Cooperative State Research Service,
Extension Service, and
National Agricultural Library—
were merged to form a new organization,
the Science and Education Administration (SEA).

New series are being established by SEA and will be sent to existing
subscribers to replace the series being discontinued.

Study conducted by
Science and Education Administration
UNITED STATES DEPARTMENT OF AGRICULTURE
In cooperation with
Minnesota Agricultural Experiment Station
and the
St. Anthony Falls Hydraulic Laboratory
University of Minnesota

CONTENTS

Hydraulic Model Investigation
For Floodwater Retarding Structure No. 3
Banklick Creek Watershed,
Boone and Kenton Counties, Kentucky

C. L. Anderson[1]

INTRODUCTION

This report describes hydraulic model studies of a two-way drop inlet closed conduit spillway for Floodwater Retarding Structure No. 3, Banklick Creek Watershed in Boone and Kenton Counties, Kentucky. The structure was designed in the Kentucky State Office of the Soil Conservation Service (SCS), U.S. Department of Agriculture.

The proposed structure was unique. Although the crest of the drop inlet was four pipe diameters (4D) long the drop inlet was 2D long, requiring a contraction section between the crest section and the drop inlet shaft. This was a significant departure from current SCS design standards in which the crest and drop inlet lengths are identical. Another departure from current practice was the use of a structural transverse wall at the midlength of the drop inlet.

The Design Branch of the Engineering Division of SCS felt the proposed design should be modeled to check its hydraulic performance.

The model study of the structure was conducted by engineers of the Science and Education Administration (SEA) at the St. Anthony Falls Hydraulic Laboratory, Minneapolis, Minn. The purposes of the model study were (1) to observe the performance and (2) to determine the flow and pressure coefficients of the drop inlet.

This report describes the proposed prototype structure and presents the reasons for departures from current design standards, and it presents the results of tests on the original design and several modifications of the spillway.

PROPOSED PROTOTYPE

A section through the proposed dam and principal spillway is shown in figure 1. The dam, to be built under the Public Law 566 program, is a floodwater retarding structure 111.9 ft high and will have a floodwater detention capacity of 1,435 acre-feet.

The proposed principal spillway has a two-way drop inlet entrance, a 4.5-ft diameter barrel, and a U.S. Bureau of Reclamation Type VI energy dissipator at the exit. The crest of the drop inlet is at elevation 617.5, 70 ft 0 in above the invert of the barrel
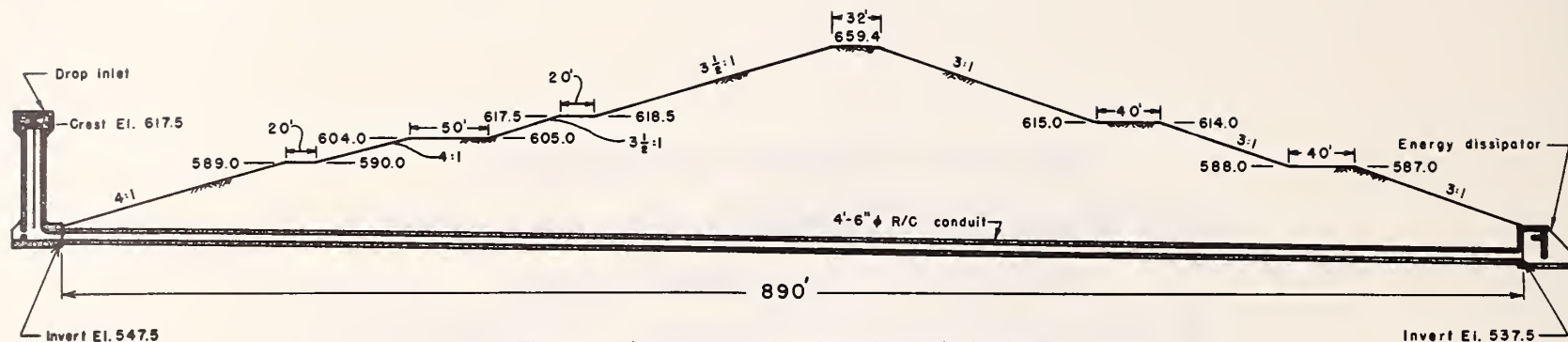
Figure 1.—Centerline section through principal spillway.

2

entrance (elevation 547.5). The design capacity of the spillway is 690 ft³/s when the pool level is at the crest of the emergency spillway (elevation 640.0), which is 98 ft above the design tailwater level (elevation 542.0) at the energy dissipator.

Figure 2 shows the geometry of the proposed drop inlet. In cross section the drop inlet flow area is 4 ft 6 in (1**D**) wide by 9 ft 0 in (2**D**) long, but is divided by the transverse splitter wall into two 4 ft 6 in (1**D**) square shafts. Although the 2D-long drop inlet is hydraulically adequate, to carry the design flow the crest and trashrack had to be 4**D** long to meet the trashrack maximum velocity criterion of 2 ft/s. Instead of using a 4D-long drop inlet for the full height, which would be subject to uplift instability as well as uneconomical, the designers proposed a 45° contraction section to join the 4D-long crest to the 2D-long drop inlet.

The crest profile is a double radius compound curve intended to prevent separation of the nappes from the weir crests and the associated nappe instability.

Longitudinally a splitter wall extends the length of the crest section. Vertically the splitter wall extends from the bottom of the antivortex plate to 1 ft 9 in below the crest over the two shafts and to the 45° endwalls of the contraction as shown in figure 2. The longitudinal splitter wall is intended to prevent the weir nappes and the boils—the rolling water supported on the nappes just before priming—from interacting and sloshing from side to side between the crests during weir flow. This sloshing could

induce oscillation of the drop inlet.

Because the designers felt that the turbulence generated during plate control might induce undesirable vibrations of the structure, the antivortex plate was located 4 ft 2 in (0.93D) above the crests to avoid plate control. This plate level is above the elevation of the intersection of the weir and pipe flow head-discharge curves, that is, above the headpool elevation at which plate control occurs.

The trashrack, consisting of vertically overlapped channel sections and known as the stepped baffle trashrack, prevents floating debris from entering the drop inlet. This trashrack design was proposed by SCS and developed by SEA in Stillwater, Okla.[2]

The transverse splitter wall at the drop inlet midlength is a structural member which reduces the unsupported length of the sidewalls. The transverse wall extends down to within 6 ft of the invert, 2 ft 1 in below the beginning of the curvature of the elbow.

A double radius elbow and a conical transition are used to join the drop inlet and the circular conduit. The elbow consists of two 45° arcs of 2 ft 3 in (D/2) and 6 ft 9 in (3D/2) radii, respectively, and is 5 ft 5 in (1.207D) long. The transition consists of a quarter section of a conical surface in each corner and is 9 ft 0 in (2D) long.

[2] Gwinn, W. R. Stepped baffle trash rack for drop inlets. Science and Education Administration, U.S. Department of Agriculture, Stillwater, Okla. Transactions, American Society of Agriculture Engineers, vol. 19, no. 1, pp. 97-104, 107. 1976.

THE MODEL

The model study was limited to investigation of the hydraulic characteristics and the performance of the two-way drop inlet. Because it would not affect the hydraulics of the inlet, the gate on the upstream end of the drop inlet was not modeled. Also, the stilling basin at the pipe spillway exit was not modeled because it would have no effect on the performance of the inlet other than influencing the rate of discharge at which various flow phenomena occur.

An existing model test facility was used. Its transparent barrel was 2.25 inches in diameter. This made the model-prototype scale ratio 1:24. The 890 ft (197.8D)-long prototype barrel slopes 1.12 percent (sine definition) beginning just downstream of the conical transition. The same barrel slope was used in the model. The model barrel, however, was only 98D long and was shorter than needed to correctly simulate the prototype barrel friction
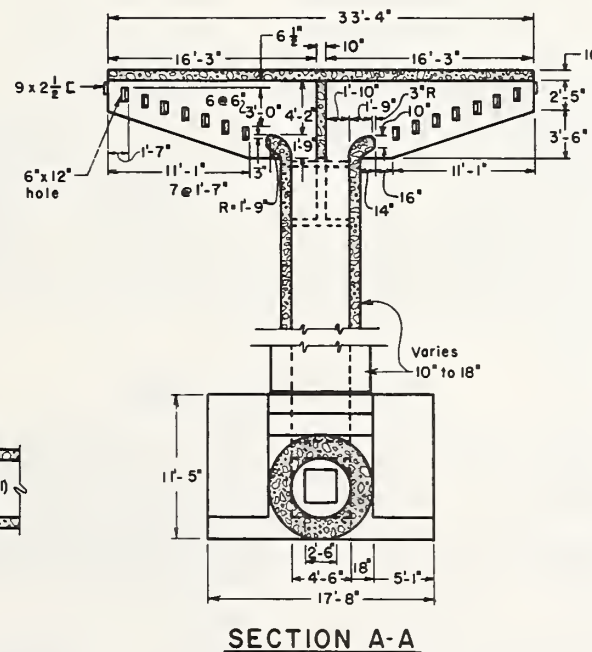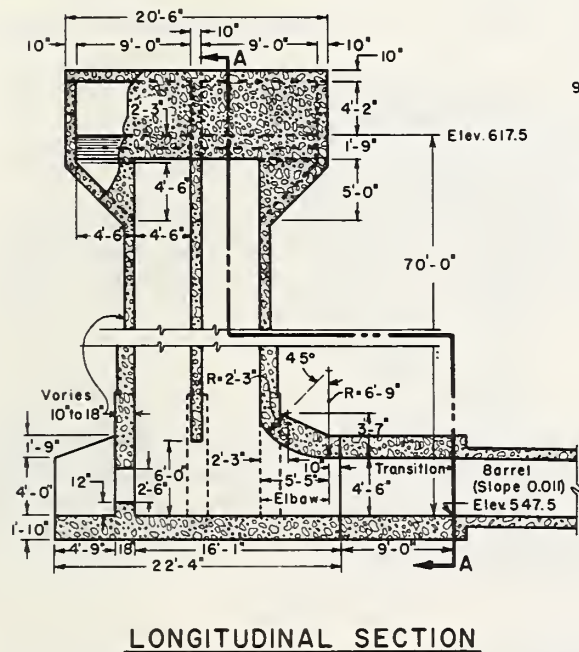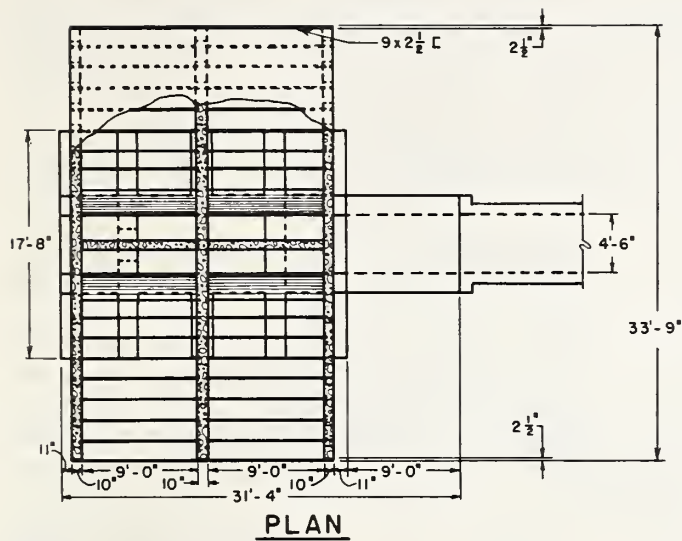
3

Figure 2.—Proposed prototype two-way drop inlet.

loss at the design discharge of 690 ft³/s. This insufficient model barrel length introduced model-prototype discrepancies in discharges greater than the priming discharge, but did not affect model performance—the main point of concern in this study.

The drop inlet itself was modeled as proposed except for two changes.[3] The inverts of the drop inlet, the elbow, and the transition were made semicylindrical rather than flat as proposed because an existing conical transition with a semicylindrical invert was available, saving considerable construction time and expense. Also, the semicylindrical invert is the SCS standard design for the two-way drop inlet. As shown in figure 3, this geometry extends the invert of the barrel upstream into the drop inlet so a transition is required only for the upper half of the cross section at the elbow exit.

The other change was the termination of the transverse splitter wall at the beginning of the elbow curvature, 2 ft 1 in above the proposed termination. This change was made because the investigators, from their experience with elbow design, felt that the elevation of the beginning of the elbow curvature was the minimum elevation of the transverse wall that could be tolerated to prevent severe restriction of the flow from the upstream shaft as the flow from the two shafts mixed and turned into the elbow. The transverse wall and the longitudinal splitter wall were made removable so that further modifications would be possible after initial testing.

All drop inlet dimensions, shown in figure 3, were modeled to scale except for the thickness of the exterior walls and the trashrack bars. Because the exterior wall thickness would not affect performance, stock thicknesses of plastic were used; however, all interior walls were machined to scale thickness. The trashrack bars were made from an extruded plastic channel section 0.375 by 0.094 in. This section scaled the depth of the prototype trashrack bars exactly, but the width should have been 0.104 in instead of 0.094 in—an insignificant difference.

The piezometers used to measure the pressures in the drop inlet, elbow, transition, and barrel entrance are numbered in figure 3:

1 and 2 are in the sidewall at the midheight and midlength of the downstream and upstream shafts of the drop inlet, respectively;

3 is in the endwall 0.1 in (0.04D) below the bottom of the downstream 45° sloping endwall and midway between the outside wall and the longitudinal splitter wall;

4 is in the sidewall above the center of the downstream shaft 0.05 in (0.02D) below the point of tangency of the crest curve with the sidewall;

5 is at the top of the crest 1.125 in (D/2) from the downstream end of the crest;

6 is in the elbow crown 2.15 in (0.96D) downstream from the elbow entrance;

7 is 0.11 in (0.05D) downstream from the transition exit and pipe entrance at 45° above the horizontal; and,

8 is in the invert of the barrel 0.56 in (0.25D) downstream of the break in the conduit alignment.

Piezometers were also used along the invert of the barrel to determine the hydraulic gradeline and friction loss in the barrel. These piezometers were located at 10D intervals beginning 13.2D downstream from the barrel entrance.

TEST PROGRAM

After initial testing and analysis had been completed on the original model, figure 3, SCS personnel involved in the prototype design and its approval came to observe and discuss the model performance. As a result of these discussions, additional performance tests were suggested. The five model conditions tested were as follows:

Series	Test Conditions
W-650........	Original model
W-651........	Original model without longitudinal wall

---

[3] Soil Conservation Service engineers later made the following changes to the drop inlet to be installed:

    1. A berm of earthfill 26 ft in height was added around the drop inlet.

    2. The transverse splitter wall was terminated at the beginning of the elbow curvature.

    3. The invert of the drop inlet and elbow was made semicylindrical.

With these changes, the original model represents the drop inlet to be installed.
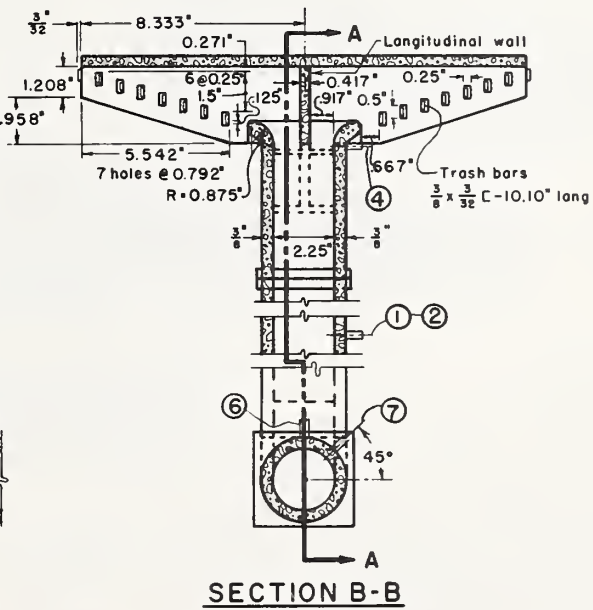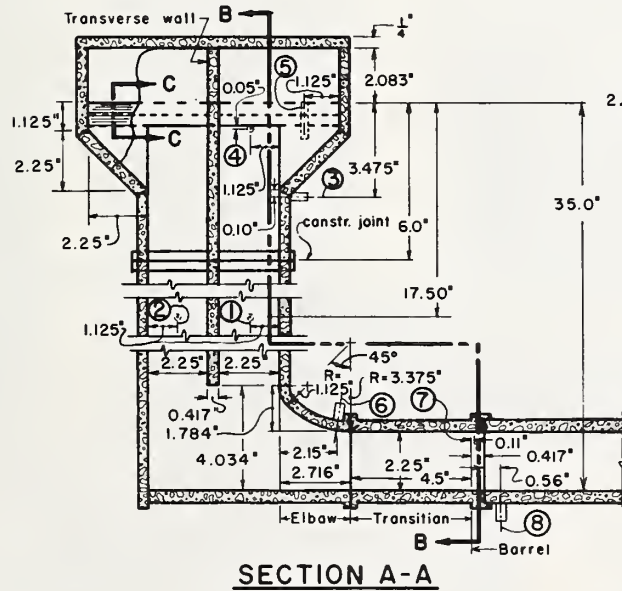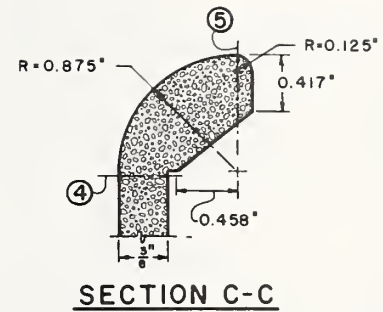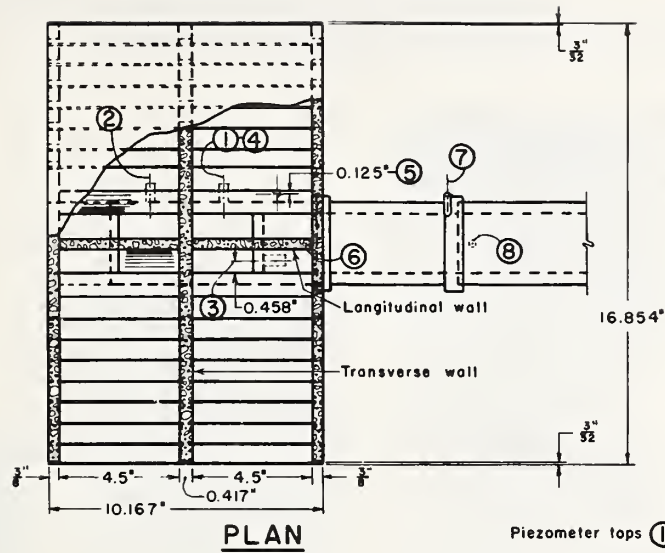
Figure 3.—Original model two-way drop inlet.

W-652 . . . . Original model with bottom of transverse wall raised **D**/2
W-653 . . . . Original model with bottom of transverse wall raised 1**D**
W-655 . . . . Original model with curved bottom extension on transverse wall

The test results for each model condition were analyzed as soon as the measurements were made to determine if further modifications and tests were needed.

TEST RESULTS

As pointed out earlier the model did not correctly simulate the prototype for pipe flow discharges. Therefore, although the flow conditions that occurred in the model as the drop inlet primed and during pipe flow can be expected to occur in the prototype, they will occur at different discharges than those represented in the model. The flow conditions during weir flow, however, were modeled as they will occur in the prototype.

Original model condition

Head-discharge data for the original model, expressed in prototype quantities, are plotted as triangles (△) in figure 4. The head-discharge relationship is unique and reversible; flow control passed directly from weir to full-pipe for rising stages and directly from full-pipe to weir for falling stages. The antivortex plate exercised no control over the head-discharge relationship because the antivortex plate was intentionally placed above the elevation of the intersection of the weir and pipe flow curves. The weir at the crest of the drop inlet controlled the head-discharge relationship up to a discharge of 642 ft³/s. The entrance loss, defined as the head loss between the headpool surface and the barrel entrance, averaged 0.20 barrel velocity heads.

During the lowest weir flows, the nappes clung to the crest and sidewall of the drop inlet. Flow over the ends of the crests dropped directly onto the sloping endwalls and concentrated along either side of the longitudinal splitter wall. Below the contraction the flow clung to the endwalls and the transverse splitter wall of the drop inlet as shown at a discharge of 38 ft³/s in figure 5,A, which shows the lower 12**D** of the 15.6**D** high drop inlet. The weir flow over the crest was attracted by surface tension to the transverse splitter wall and the endwalls so there is no flow on the sidewalls in figure 5,A. The prototype, however, would probably not perform this way. At a slightly higher weir flow of 73 ft³/s, the surface tension effects disappeared and the flow was attached to all four walls in each shaft.
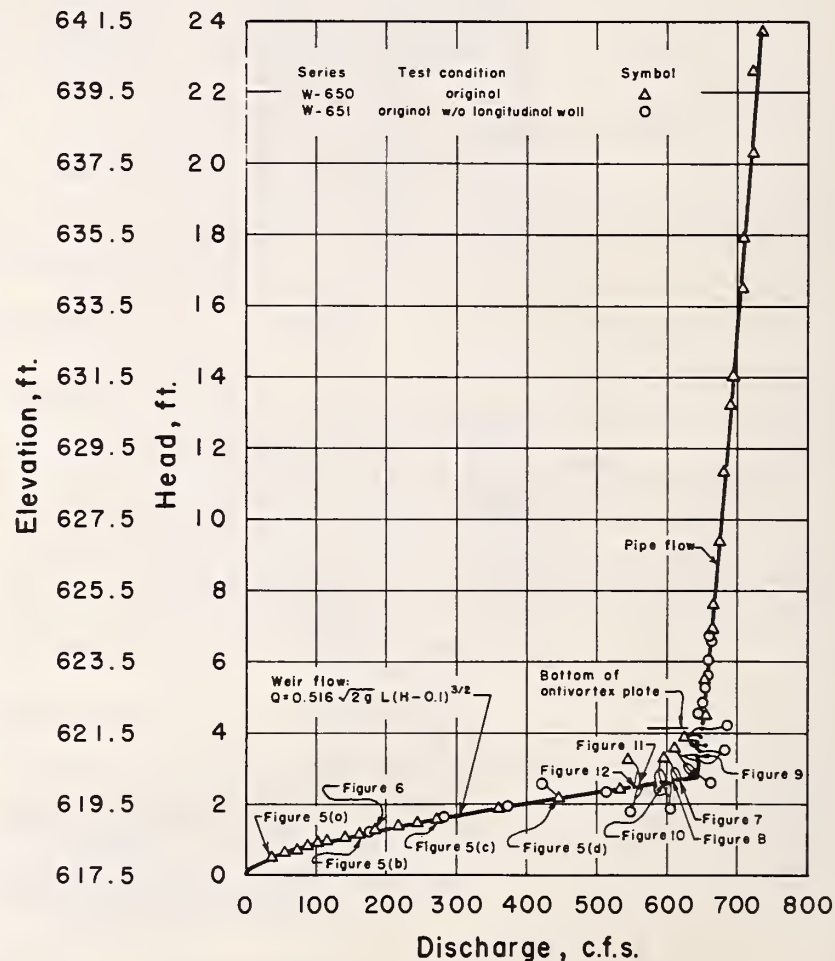

Figure 4.—Model head-discharge relationships: original design with and without longitudinal wall.
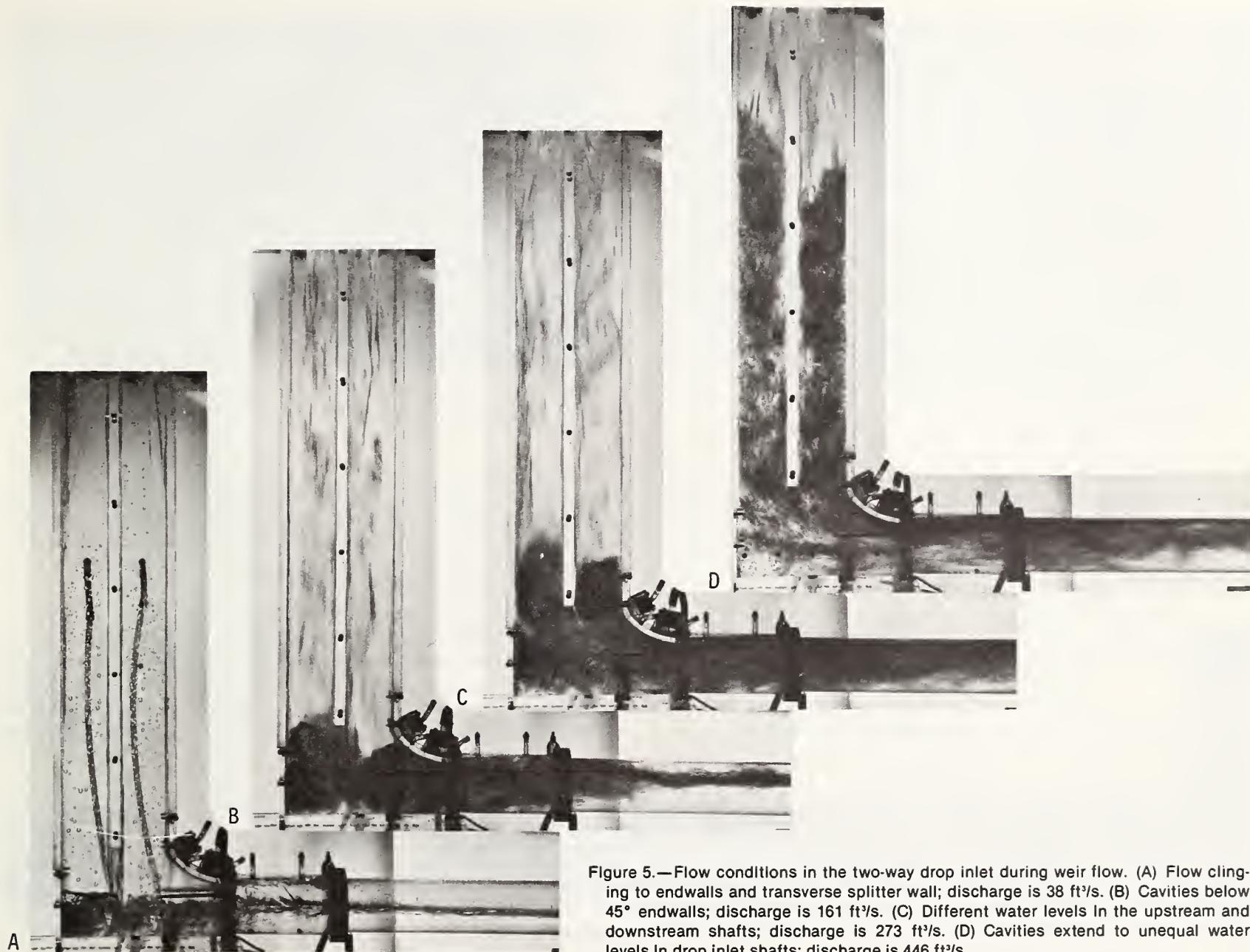
Figure 5.—Flow conditions in the two-way drop inlet during weir flow. (A) Flow cling-ing to endwalls and transverse splitter wall; discharge is 38 ft³/s. (B) Cavities below 45° endwalls; discharge is 161 ft³/s. (C) Different water levels In the upstream and downstream shafts; discharge is 273 ft³/s. (D) Cavities extend to unequal water levels In drop inlet shafts; discharge is 446 ft³/s.

With further increase in flow the jets from the sloping endwalls separated from the shaft endwalls at the bottom of the contraction. The cavity formed under the jet in each shaft for a flow of 161 ft³/s is shown in figure 5,B. The separated jets forced the flow just below the contraction into about the center two-thirds of the drop inlet length. However, by midheight the flow expanded to fill the shaft.

The drop inlet flow conditions at a discharge of 185 ft³/s were similar to those just described, but the spillway sealed intermittently at the elbow entrance causing traveling slugs in the barrel. A traveling slug of water, which fills the barrel just downstream of the barrel midlength, is shown in figure 6. However, because the crest weirs controlled the head-discharge relationship, these slugs had no effect on the head-discharge relationship.

8   As the flow was increased further the water level in the drop inlet rose, the flow in the drop inlet became more turbulent, and the barrel filled with an air-water mixture for increasing distances.

A difference between the water levels in the upstream and downstream shafts of the drop inlet became apparent at a discharge of 273 ft³/s. The level in the downstream shaft was lower than the level in the upstream shaft, as shown in figure 5,C. This resulted from unequal head losses associated with the junction of shaft flows at the base of the drop inlet.
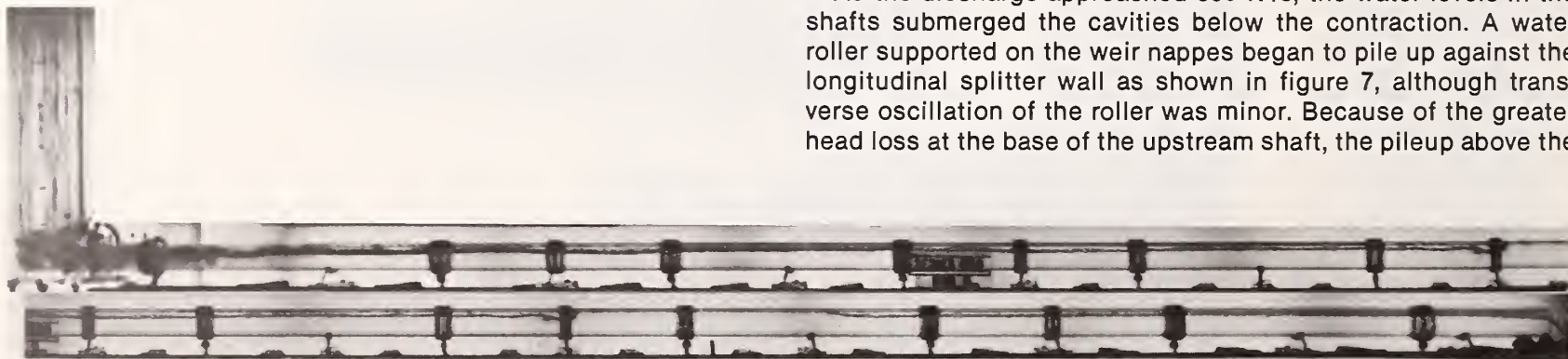

Figure 7.—Crest flow condition just before priming of drop inlet; discharge is 619 ft³/s. Weir nappes support water roller against longitudinal splitter wall.

With still further increases in the flow, the water levels in the drop inlet continued to rise and the length of the cavities below the contraction increased. As shown in figure 5,D, at a discharge of 446 ft³/s the cavities extended to the water levels in the drop inlet, which are just above the midheight. At this flow there were always slugs in the barrel.

As the discharge approached 600 ft³/s, the water levels in the shafts submerged the cavities below the contraction. A water roller supported on the weir nappes began to pile up against the longitudinal splitter wall as shown in figure 7, although transverse oscillation of the roller was minor. Because of the greater head loss at the base of the upstream shaft, the pileup above the

Figure 6.—Flow condition in the barrel; discharge is 185 ft³/s. A slug formed at the barrel entrance and its head has moved downstream to 58D. (The upper section shows the bottom of the drop inlet and the barrel from 0D to 61D, the lower section shows the barrel from 35D to its exit—98D.)

upstream shaft began at a lesser flow than the pileup above the downstream shaft. This resulted in a slightly higher water level above the upstream shaft, which is also evident in figure 7. As a result there was less air entrainment in the upstream shaft than in the downstream shaft for a given discharge, as shown by the bubbles in figure 8.

With further increase in the discharge the air flow gradually decreased. The air flow stopped and the spillway flowed full of water at a discharge of 643 ft³/s. However, as pointed out previously, this priming discharge is not quantitatively correct for the prototype. Although rough and turbulent, the water surface

Figure 9.—Crest flow condition at priming; discharge is 643 ft³/s.

9

over the drop inlet, particularly over the upstream shaft, was almost level with the pool surface as shown in figure 9.

During pipe flow, pressure differences of up to 5.25 ft or $0.17h_{vp}$ (0.17 barrel velocity heads) were measured between the mid-height of the two shafts. These pressure differences indicated that differences in the head losses at the base of the' shafts prevailed throughout the pipe flow range of discharges.

Because the head-discharge curve was unique and reversible, the flow conditions described above occurred similarly, but in reverse order, as the discharge was decreased.

Original model without longitudinal wall

For structural reasons the longitudinal splitter wall has to be at least 10 inches thick. This reduces the clear space between the longitudinal wall and the drop inlet sidewall and, particularly on installations having small conduits, impedes or prevents access to the drop inlet for inspection and maintenance. Also, to avoid plugging the spillway, the small clear space requires that the spacing of the trashrack bars be reduced to control the maximum size debris that can enter the inlet. For these reasons, together with the added cost for its construction, the longitudinal wall is

Figure 8.—Difference in air entrainment in two drop inlet shafts is caused by difference in head loss between shafts; discharge is 610 ft³/s.

undesirable. However, the designers felt the longitudinal wall was necessary to prevent undesirable sloshing at the crest of this structure.

Test series W-651 was conducted to determine if the performance of the proposed drop inlet would be acceptable without the longitudinal splitter wall. As shown by the circles plotted in figure 4, the head-discharge relationship is identical to that for the original model. The entrance loss coefficient averaged 0.20, also the same as that for the original model.

Flow conditions throughout much of the test range were similar to those for the original model. However, just before weir flow at the crest became submerged, a nappe-supported boil developed between the opposing nappes as shown in figure 10. This boil sloshed from side to side, rebounding from nappe to nappe. The boil was also observed with the longitudinal wall in place but, although the boil piled up against the wall, the wall prevented its oscillation.

Figure 11.—Air entrainment during weir flow without the longitudinal splitter wall; discharge is 560 ft³/s. Large air pockets entrained with high concentration of small bubbles.

Downstream

Figure 10.—Weir flow condition without the longitudinal splitter wall; discharge is 595 ft³/s. A boil developed between the opposing nappes, which oscillated from side to side.

In addition to the steady flow of small air bubbles observed both with and without the longitudinal wall in place, much larger pockets of air were occasionally entrained at the crest and carried down the inlet when the longitudinal wall was removed. At a discharge of 560 ft³/s, several large air pockets flowed down the shafts as shown in figure 11.

With the exception of boil oscillation and increased air pocket size, the performance of the spillway without the longitudinal wall was similar to that of the spillway with the longitudinal wall.

Original model with bottom of transverse wall raised D/2 and 1D

The pressure difference and the unequal water levels in the upstream and downstream shafts of the drop inlet for the original model were considered undesirable. These pressure and water level differences were caused by constriction of the flow from the upstream shaft by the downstream shaft flow and by the bottom of the transverse splitter wall. Figure 12 illustrates the sharp bend the flow from the upstream shaft makes at the bottom of the

Figure 13.—Model head-discharge relationships with transverse splitter wall modifications.

Figure 12.—Flow condition at base of drop inlet with original design; discharge is 555 ft³/s. Constricted flow in upstream shaft deflects downstream abruptly at the bottom of the transverse splitter wall.
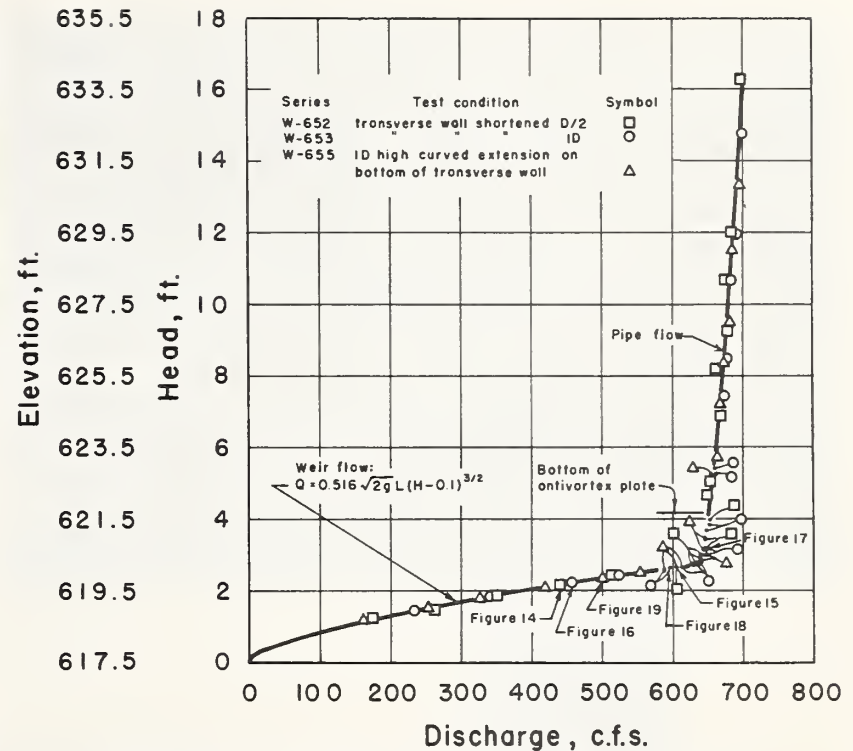
transverse wall with the original design. The flow pattern is indicated by the distribution of air bubbles and by the deflection of the cavity at the bottom of the transverse wall.

The flow pattern indicated that raising the bottom of the transverse wall might alleviate the problem by allowing the flow from the upstream shaft more favorable access to the conduit entrance. This hypothesis was tested by progressively shortening the transverse splitter wall.

The bottom of the transverse wall was first raised D/2 for test series W-652. Head-discharge data for this test, plotted as squares (□) in figure 13, are identical to the data for the original model.

Flow conditions were similar to those observed for the original model. The water level in the upstream shaft was still higher than in the downstream shaft as shown in figure 14,A. The reason for this becomes obvious at a higher rate of water flow: the deflection of the air bubbles and the cavity at the bottom of the shortened transverse wall, shown in figure 14,B, indicates that the flow from the upstream shaft was still constricted.

Midheight pressures measured in each shaft during full-pipe flow indicated a maximum pressure differential of 2.9 ft or $0.09h_{vp}$. This difference is nearly half the 5.25 ft or $0.17h_{vp}$ measured in the original model. The average entrance loss coefficient was 0.19, also slightly reduced from the previous value of 0.20. These figures indicate that shortening the transverse splitter wall D/2 is beneficial.

To further reduce the pressure difference, the transverse wall was again shortened D/2 for series W-653 to raise its bottom 1D above that of the original model. Head-discharge data for this test, plotted as circles (O) in figure 13, are again identical to the data for the original model. Flow conditions were also similar except that, as shown in figure 15,A, the water surfaces in both drop

Figure 14.—Flow conditions in the two-way drop inlet with the bottom of the transverse splitter wall raised D/2. (A) Water level is still higher in the upstream shaft than in the downstream shaft; discharge is 441 ft³/s. (B) Flow from upstream shaft still deflects downstream abruptly at the base of the transverse splitter wall; discharge is 605 ft³/s.
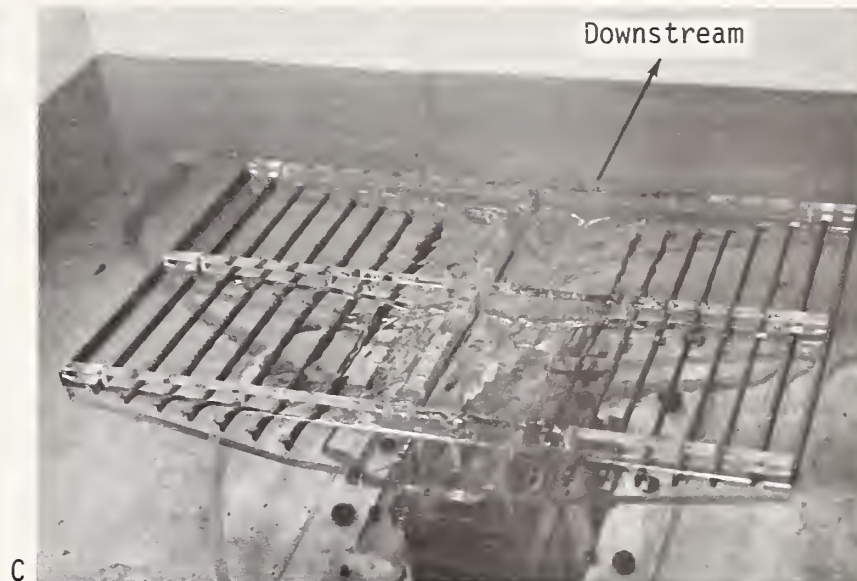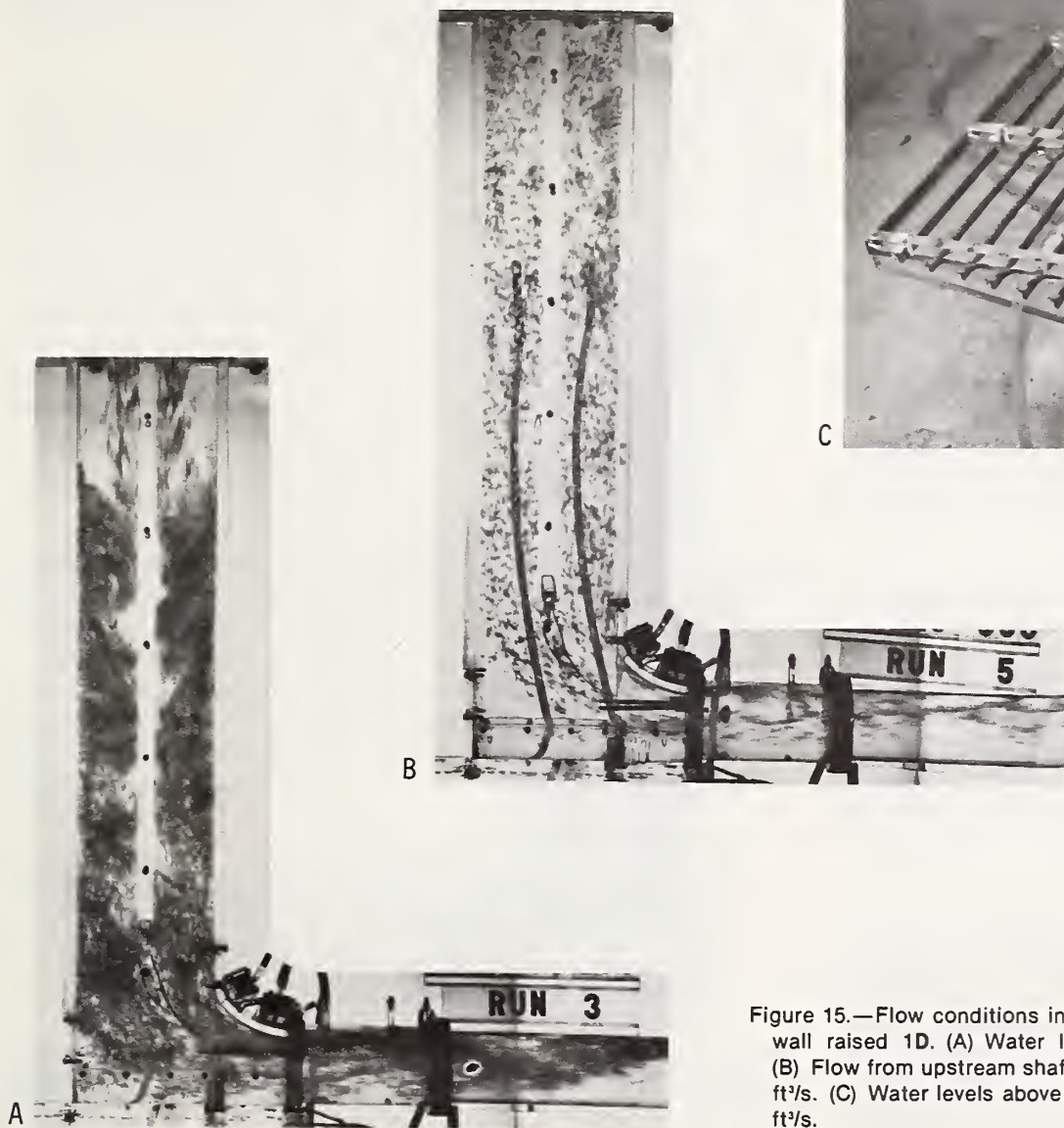
Downstream

13

Figure 15.—Flow conditions in the two-way drop inlet with the bottom of the transverse wall raised 1D. (A) Water levels are equal in both shafts; discharge is 458 ft³/s. (B) Flow from upstream shaft exits tangent to transverse splitter wall; discharge is 596 ft³/s. (C) Water levels above both shafts are equal just after priming; discharge is 650 ft³/s.

inlet shafts were essentially at the same level. Identical crest conditions over each shaft are illustrated in figure 15,C.

The flow pattern at the base of the drop inlet is illustrated in figure 15,B—the cavity is gently curved and tangent to the transverse wall and the air bubbles are more uniformly distributed across the elbow entrance. The dark lines on the drop inlet sidewall outline the cavity and downstream flow lines for the transverse wall shortened **D/2** for comparison with the cavity and flow lines shown by bubbles for the wall shortened **1D**.

The entrance loss coefficient decreased to 0.18 for the transverse wall shortened **1D**, a decrease of 0.02 from that for the original wall. The midheight pressures measured during pipe flow indicated a maximum pressure difference of 1.4 ft or $0.05h_{vp}$. Although head losses still were not quite equal in the two shafts, their difference was considered to be relatively minor and would need no further reduction. This $0.05h_{vp}$ pressure differential is a considerable reduction from the $0.17h_{vp}$ reported for the original wall length and the $0.09h_{vp}$ reported for the **D/2** shortened wall.

The hydraulic performance of this structure with the bottom of the transverse wall raised **1D** above the beginning of the elbow curvature was completely acceptable.

Original model with curved extension on bottom of transverse wall

Although the hydraulic performance was improved by shortening the transverse splitter wall, it had been achieved at the expense of a **1D** reduction in the structural support length between the sidewalls of the drop inlet. This was undesirable. Adequate sidewall support down to the beginning of the elbow curvature and approximate flow equality in the two shafts could be obtained simultaneously by curving an extension of the transverse wall in the downstream direction.

The cavity streamline extending from the upstream edge of the bottom of the transverse wall in figure 15,B was used to determine the proper curvature of the wall extension. The streamline was approximated by an arc with a prototype radius of 10 ft (2.22D). In the model a curved wall section of 2.22D outer radius and the same thickness as the transverse wall was added to the shortened wall of the previous test. The bottom of the curved ex-

tension was terminated at the elevation where the elbow curvature begins.

Model tests of this wall configuration (series W-655) produced a head-discharge relationship, plotted as triangles (△) in figure 13, identical to those for the various wall lengths tested in series W-650, W-652, and W-653. Flow conditions were similar to those with the transverse wall shortened **1D**.

The entrance loss coefficient averaged 0.19. For comparison, the entrance loss coefficients for the wall shortened **1D**, the wall shortened **D/2**, and for the original transverse splitter wall were 0.18, 0.19, and 0.20.

Figure 16.—Flow in the two-way drop inlet with the curved extension on the bottom of the transverse splitter wall; discharge is 500 ft³/s. Water level in downstream shaft is slightly higher than in upstream shaft.

14

The maximum pressure difference in the two drop inlet shafts was only 0.7 ft or $0.02h_{vp}$, half that obtained for the wall shortened 1D and one-eighth that for the original transverse wall. As shown in figure 16, the water level in the downstream shaft was slightly above that in the upstream shaft, so the difference in head loss was reversed from that observed during previous test series.

Although the curved transverse wall extension slightly overcompensated the disparity in head loss, the effect was minor because the two shafts primed almost simultaneously.

ANALYSES OF RESULTS

Weir Flow

Previous analyses[4] of the general weir flow head-discharge relationship, $Q = CLH^{3/2}$, show that H is linearly related to $Q^{2/3}$. Here Q is the discharge, C is the weir discharge coefficient, L is the weir length, and H is the head on the weir. This implies that the weir discharge coefficient is a constant. However, a plot of H versus $Q^{2/3}$ shows that, with C assumed constant, a head correction is necessary to make the line representing the data pass through the origin of coordinates.

For the Banklick Creek model data, the head-discharge relationship derived on this basis is

$$Q = 4.14\, L(H - 0.1)^{3/2} = 0.516\, \sqrt{2g}\, L(H - 0.1)^{3/2} \qquad (1)$$

where g is the acceleration of gravity and L, H, and 0.1 are in feet prototype scale. The agreement between the data and equation 1 is indicated in figures 4 and 13.

Without the head correction, the discharge coefficient varies from 2.90 at low weir heads to 4.10 at high weir heads. When the head correction is included in equation 1, the discharge coefficient becomes constant and the agreement between the equation and the data is good.

Full-conduit flow

Pipe flow is defined by the relationship

$$Q = \frac{\pi D^2}{4} \sqrt{\frac{2gH_t}{K_e + K_o + f\ell/D}} \qquad (2)$$

[4] Blaisdell, F. W., and Donnelly, C. A. Capacity of box inlet drop spillways under free and submerged flow conditions. St. Anthony Falls Hydraulic Laboratory, University of Minnesota, Minneapolis. Tech. Paper No. 7, Series B. January 1951.

where Q is the discharge,
- D is the barrel diameter,
- H_t is the total head available,
- K_e is the entrance loss coefficient,
- K_o is the outlet loss coefficient ($K_o = 1$),
- f is the Darcy-Weisbach friction factor for the barrel, and
- ℓ is the length of the barrel.

The model head H_t, friction factor f, and barrel length ℓ are not similar to corresponding prototype elements so prototype values must be used to compute the discharge. However, because the model drop inlet geometry is similar to the prototype geometry, the entrance loss coefficient K_e is the same for both model and prototype. Values of K_e obtained for each drop inlet configuration tested are listed in table 1.

Table 1 shows that the entrance loss is reduced 5 percent by shortening the transverse wall D/2 or by adding a curved extension to the transverse wall. Shortening the transverse wall 1D reduced the entrance loss by 10 percent from the original value. However, all values of K_e are so small that the entrance loss for the Banklick Creek structure is a relatively small part of the total loss.

Drop inlet pressures

The five locations in the drop inlet where pressures were measured are shown in figure 3 and are described under the heading "THE MODEL."

The drop inlet pressure data are expressed in dimensionless form as a pressure coefficient, h_n/h_{vp}, where h_n is the local pressure head relative to the head at the same elevation in the pool outside the drop inlet and h_{vp} is the velocity head in the barrel. Average values of h_n/h_{vp} for each test series are listed in table 1.

TABLE 1.—*Entrance loss and pressure coefficients for the drop inlet*

Series	Drop inlet geometry	Entrance loss coefficient, K_e	h_n/h_{vp} Piezometer				
			1	2	3	4	5
W-650	Original	0.20	− 0.30	− 0.13	− 0.46	− 0.17	− 0.10
W-651	Without longitudinal wall	.20	− .30	− .13	− .46	− .13	− .09
W-652	Bottom of transverse wall raised D/2	.19	− .26	− .17	− .41	− .16	− .09
W-653	Bottom of transverse wall raised 1D	.18	− .23	− .19	− .37	− .14	− .08
W-655	Curved bottom extension on transverse wall	.19	− .20	− .22	− .32	− .13	− .07

Prototype pressure heads will be given when the pressures at each drop inlet piezometer are discussed.

Pressure data for piezometers 1 and 2, located at the midheight of the downstream and upstream drop inlet shafts, respectively, are listed in table 2. The pressure coefficient h_n/h_{vp}, the differences between the pressure coefficients in the two shafts, the pressure head relative to that in the pool outside the drop inlet h_n, and the actual pressure head at the piezometer h_p are tabulated for these piezometer locations for each test condition. The two values of discharge for each drop inlet geometry shown in table 2 are actual test values corresponding approximately to the model priming discharge (in terms of prototype scale) and the prototype design discharge, respectively.

TABLE 2.—*Pressure at midheight of drop inlet*

Drop inlet geometry	h_n/h_{vp} Piezometer			Discharge	h_n Piezometer		h_p Piezometer	
	1	2	1-2		1	2	1	2
				ft³/s	ft	ft	ft	ft
Original	− 0.30	− 0.13	− 0.17	643	− 8.2	− 3.7	30.2	34.7
				691	− 8.9	− 3.9	39.3	44.3
Bottom of transverse wall raised D/2	− .26	− .17	− .09	639	− 7.1	− 3.8	30.9	34.2
				699	− 7.7	− 4.9	43.6	46.4
Bottom of transverse wall raised 1D	− .23	− .19	[1]− .05	648	− 6.4	− 5.2	31.6	32.8
				701	− 6.9	− 5.7	42.8	44.0
Curved bottom extension on transverse wall	− .20	− .22	+ .02	644	− 5.4	− 6.4	32.6	31.6
				698	− 6.2	− 6.7	42.1	41.6

[1] Difference before rounding 1 and 2.

For the original drop inlet geometry, the pressure head in the downstream shaft was lower than that in the upstream shaft by $0.17h_{vp}$, or about 5 ft. The actual pressure head at the drop inlet midheight exceeded 30 ft for all pipe flows. The pressure heads relative to that in the pool outside the drop inlet are negative— about − 9 ft in the downstream shaft and − 4 ft in the upstream shaft.

As the transverse wall was successively shortened and finally the curved extension added at its bottom, the pressure difference between the drop inlet shafts diminished. With the transverse wall shortened D/2 the pressure head difference was reduced to $0.09h_{vp}$, or about 3 ft. With the transverse wall 1D shorter than for the original geometry, the pressure head was $0.05h_{vp}$ or 1.2 ft lower at the midheight of the downstream shaft than at the midheight of the upstream shaft. Actual pressure heads at the midheight piezometers remain in the 31 to 44 ft range over the range of discharges.

When the transverse wall was extended vertically downward 1D by means of a cylindrical arc with an upstream radius of 10 ft or 2.22D, the difference in pressure between the shafts reversed with the midheight pressure head in the downstream shaft being $0.02h_{vp}$, or about 1 ft, higher than that in the upstream shaft. This pressure difference between the two shafts probably is an insignificant loading of the transverse splitter wall. The actual pressure heads were about 32 ft at priming discharge and 42 ft at design flow. The pressure head across the exterior walls at the drop inlet midheight was about − 6 ft.

Piezometers 3, 4, and 5 were located in the downstream shaft and were affected by the changes made on the bottom of the transverse wall in the same way that these changes affected the pressure at piezometer 1.

Table 3 lists the pressure data at piezometer 3 located near the top of the downstream shaft just below the sloping endwall. As the bottom of the transverse wall was successively raised D/2 and 1D and finally the curved extension added, the pressure at the top of the shaft successively increased until it reached a value about 30 percent above the value for the original transverse wall. The actual pressure head, h_p, also increased, but remained negative at the priming discharge until the curved extension was added.

16

TABLE 3.—*Pressures in downstream shaft below sloping endwall*

Drop inlet geometry	h_n/h_{vp}	Discharge	h_n	h_p
		ft^3/s	ft	ft
Original	−0.46	643	−13.0	−2.5
		691	−13.2	+7.0
Bottom of transverse wall raised D/2..........	−.41	639	−11.0	−0.9
		699	−12.0	+11.4
Bottom of transverse wall raised 1D	−.37	648	−10.2	−0.1
		701	−10.8	+11.1
Curved bottom extension on transverse wall ...	−.32	644	−9.2	+0.8
		698	−9.5	+10.9

TABLE 5.—*Effect of longitudinal wall on weir crest pressures*

Drop inlet geometry	h_n/h_{vp} Piezometer 4	5	Discharge	h_n Piezometer 4	5	h_p Piezometer 4	5
			ft^3/s	ft	ft	ft	ft
Original	−0.17	−0.10	643	−4.8	−3.9	+0.4	−0.5
			666	−4.8	−2.9	+4.7	+4.7
Without longitudinal wall	−.13	−.09	644	−4.1	−4.3	+1.1	−1.0
			665	−3.3	−2.6	+5.1	+4.0

Table 4 lists pressure data for piezometers 4 and 5, located in the crest region of the downstream shaft. Pressure coefficients at both locations, affected by the successive changes made in the bottom of the transverse wall, successively increased until they reached a value about 25 percent above the value for the original transverse wall. Actual pressure heads, h_p, and relative pressure heads, h_n, varied above and below the values for the original transverse wall but increased overall as the transverse wall was successively modified.

Table 4 shows that in the crest region the pressure head was always greater just below the crest profile (piezometer 4) than on top of the crest (piezometer 5), particularly at the lower discharge. The pressure head on top of the crest was always slightly negative, $0 > h_p \geq -1.0$ ft, at the priming discharge but increased with the discharge. There was therefore no cavitation potential on the weir crest during pipe flow.

TABLE 4.—*Pressures in weir crest region at piezometers 4 and 5*

Drop inlet geometry	h_n/h_{vp} Piezometer 4	5	Discharge	h_n Piezometer 4	5	h_p Piezometer 4	5
			ft^3/s	ft	ft	ft	ft
Original	−0.17	−0.10	643	−4.8	−3.9	+0.4	−0.5
			691	−4.8	−3.2	+10.2	+10.0
Bottom of transverse wall raised D/2	−.16	−.09	639	−4.2	−4.0	+0.6	−1.0
			699	−4.6	−2.4	+13.5	+13.8
Bottom of transverse wall raised 1D	−.14	−.08	648	−4.0	−3.6	+0.8	−0.6
			701	−4.1	−2.4	+12.5	+12.4
Curved bottom extension on transverse wall	−.13	−.07	644	−3.5	−3.0	+1.3	−0.1
			698	−3.8	−2.1	+11.3	+11.2

The longitudinal wall affected the crest pressures only. Pressure data in the crest region of the original drop inlet geometry with and without the longitudinal wall are presented in table 5. Pressure heads are listed for discharges just above priming and somewhat below the design discharge because the design discharge was not reached in the test without the longitudinal wall.

Table 5 shows that the average pressure coefficient, h_n/h_p, and the relative pressure head, h_n, increased when the longitudinal wall was removed.

The actual pressure head, h_p, at the piezometers shows that when the longitudinal wall was removed the pressure increased below the crest profile (piezometer 4) but decreased at the top of the crest (piezometer 5). However, since changes in the pressures were relatively minor, ≤ 0.7 ft, the effect of the longitudinal wall on the drop inlet pressures was not significant.

Because the crest profile for this inlet was a new SCS design, the pressure on the crest was measured during weir flow also. The pressure head, h_p, at the crest piezometers was expressed in terms of the priming head for the structure, H_D, rather than a weir design head because this crest profile was not based on the nappe profile for a particular weir head. The prototype priming head for this structure is 2.67 ft above the weir crest.

Figure 17,A is a plot of the crest pressure heads at piezometers 4 and 5 for varying head on the crest during weir flow and initial pipe flow with the original model geometry. The pressure head on the weir decreased from about zero at the minimum head ($H = 0.4H_D$) for which data were available to a minimum value at and just after the priming head $H/H_D = 1$ was reached. The minimum pressure head was −2.06 ft ($h_p/H_D = -0.77$) at the bottom of the crest profile (piezometer 4) and −3.42 ft
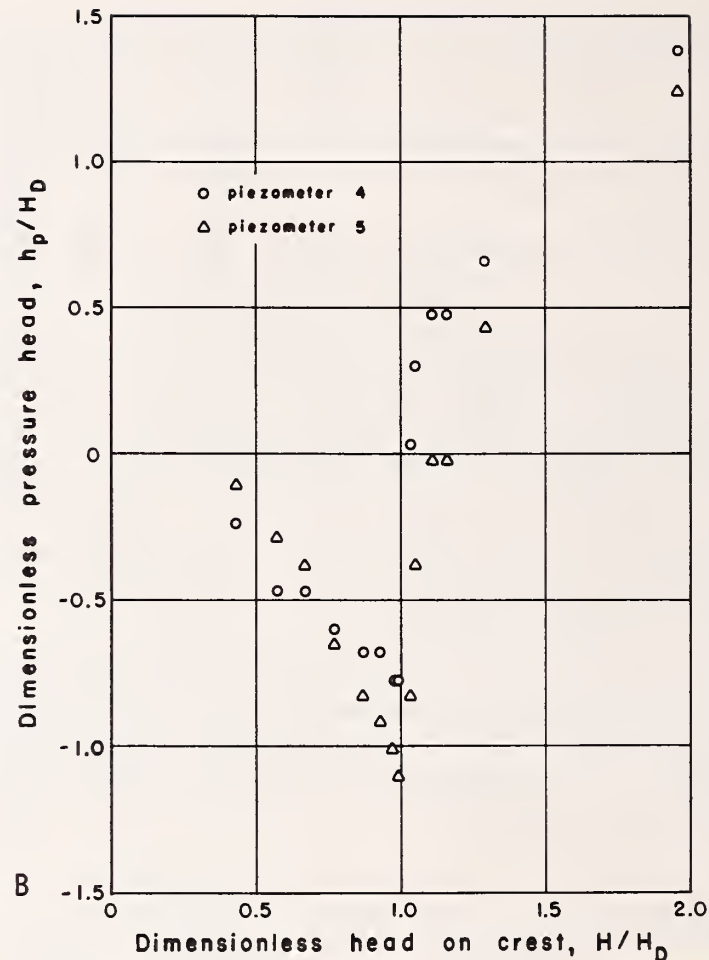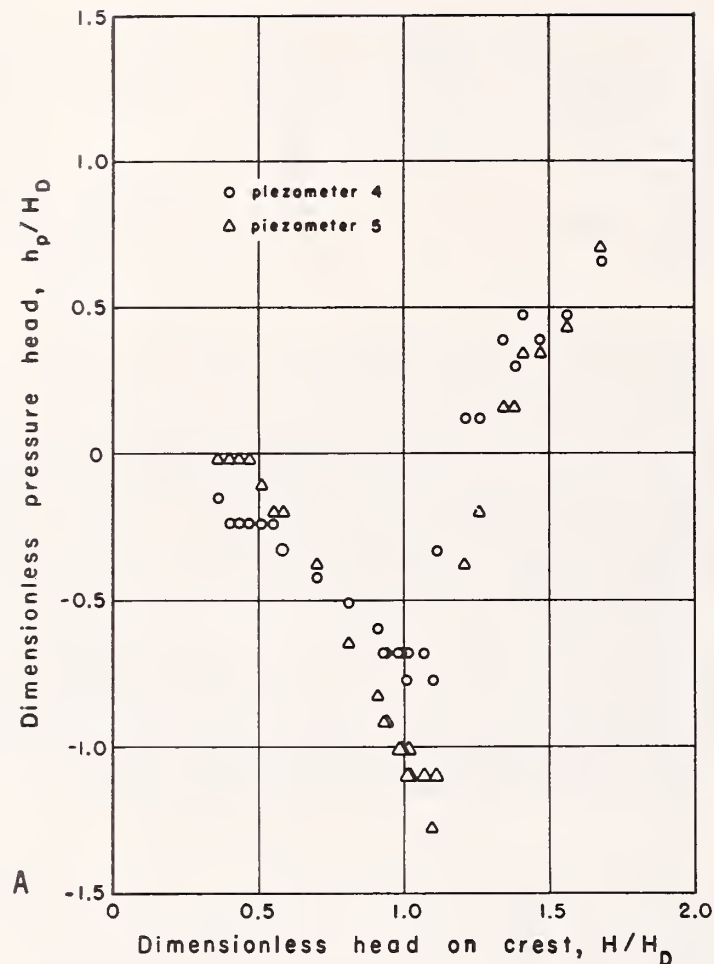
18

Figure 17.—Crest pressures during weir flow. (A) Original geometry. (B) With curved extension on transverse wall.

$(h_p/H_D = -1.28)$ on top of the crest profile (piezometer 5). The minimum pressures occurred after the pool reached the priming head. This is because the crest pressures were measured in the downstream shaft and the unequal head losses in the two drop inlet shafts caused the downstream shaft to prime later than the upstream shaft so the measured priming head is not the head

that represents flow conditions in the downstream shaft. Once priming began the weirs became submerged and the crest pressures increased rapidly.

The near-zero crest pressure at small heads and decreasing pressure as the head rises are explained by comparing the crest profile to the bottom profile of a nappe from a sharp-crested weir

under the minimum head measured. The upstream part of the crest profile was quite similar to that of the lower nappe profile for this head so the pressures should be near zero at the low heads. As the head increased however, the crest profile curvature became increasingly too sharp relative to the lower nappe surface. Thus the increasing flow separation tendency caused the crest pressures to decrease as shown in figure 17.

Modifications of the transverse wall had only a slight effect on the crest pressures. Figure 17,B is a plot of the crest pressure heads with the curved extension on the transverse wall. During weir flow the pressures were similar. The minimum pressure heads were -2.06 ft ($h_p/H_D = -0.77$) at piezometer 4 and -2.94 ft ($h_p/H_D = -1.10$) at piezometer 5 at the priming head. Because the water levels in the drop inlet shafts were equal both shafts primed simultaneously at $H/H_D = 1.0$. After priming, the pressures increased more abruptly with the curved transverse wall extension than they did with the original geometry. This is because there was less flow in the downstream shaft for a given pool level than was the case with the original geometry. With less flow in the downstream shaft the crest velocities were less and the crest pressures higher for a given pool level with the curved extension on the transverse wall.

Conduit entrance pressures

The elbow and transition are considered part of the barrel entrance. The double radius elbow and the conical transition installed in the Banklick Creek model were constructed and used during an earlier study of elbows and transitions for two-way drop inlets. The locations of minimum pressure on the elbow and the

TABLE 6.—*Average pressure coefficients in barrel entrance region*

Series	Drop inlet geometry	h_n/h_{vp} Piezometer		
		6	7	8
W-650	Original	+ 0.13	− 0.01	+ 0.06
W-651	Without longitudinal wall	+ .13	+ .00	+ .06
W-652	Bottom of transverse wall raised D/2............	+ .10	− .02	+ .04
W-653	Bottom of transverse wall raised 1D	+ .09	− .02	+ .04
W-655	Curved bottom extension on transverse wall	+ .08	− .02	+ .03

transition were determined during the original study so piezometers 6 and 7 were installed at these predetermined locations.

The inverts of the drop inlet, elbow, and transition were horizontal. The barrel sloped 1.12 percent beginning 0.185D downstream from the transition exit. The abrupt change in grade was expected to produce a low pressure region so piezometer 8 was placed in the invert of the pipe entrance as described earlier.

Pressures in the conduit and its entrance are expressed in dimensionless form as pressure coefficients, h_n/h_{vp}. However, h_n in this case is the deviation of the hydraulic gradeline from the extended friction gradeline in the barrel. Expressed in this way the pressure coefficients are valid for any geometrically similar drop inlet and barrel entrance regardless of the friction gradeline position.

Average pressure coefficients for piezometers 6, 7, and 8 are listed in table 6. Values in the table indicate that the hydraulic gradeline is above or only slightly below the friction gradeline in the barrel entrance region for all the geometries tested. Therefore, there is no cavitation potential at any point in the barrel entrance of the Banklick Creek structure.

19

RECOMMENDATIONS AND CONCLUSIONS

The performance and capacity of the Banklick Creek two-way drop inlet, as designed, were found to be generally adequate with one minor alteration. The transverse wall should extend downward no lower than the elevation of the beginning of the elbow curvature.[5] Even with the bottom of the transverse wall at this level the midheight pressure head in the upstream shaft was

---

[5] See footnote 3, page 4.

$0.17h_{vp}$ higher than that in the downstream shaft and the various stages of flow development occurred at lesser discharges in the upstream shaft than in the downstream shaft. However, these conditions did not adversely affect the hydraulic performance of the structure.

To equalize the head loss through the two shafts and eliminate the load on the transverse wall caused by unequal pressures in

the two shafts, the transverse wall should either be terminated 1**D** above the elevation where the elbow curvature begins or the bottom 1**D** length of the wall should be curved in the downstream direction with a radius of 2.22**D**, terminating at the elevation where the elbow curvature begins.

The flow into the drop inlet was disturbed by the contraction between the 4**D**-long weir crests and the 2**D**-long drop inlet. The jets from the sloping endwalls in the contraction intersected the nappes falling from the crest. However, these disturbances did not noticeably affect the performance of the structure.

The longitudinal splitter wall prevented lateral sloshing of the boil supported on the nappes as the weirs became submerged. When the longitudinal wall was removed, sloshing of the nappes occurred.

ACKNOWLEDGMENTS

NOMENCLATURE

C	weir discharge coefficient		H_D priming head
D	barrel diameter		H_t total head
f	Darcy-Weisbach friction factor		K_e entrance loss coefficient
g	gravitational acceleration		K_o outlet loss coefficient
h_n	in the drop inlet, the local pressure head relative to the pressure head at the same elevation in the pool	outside the drop inlet; for the conduit entrance, the local pressure head deviation from the extended barrel friction gradeline	ℓ length of conduit
		h_p actual pressure head	L drop inlet crest length
		h_{vp} velocity head in the barrel	Q discharge
		H head on the drop inlet crest	

GPO 820-136-1